

Review

The Polarized Emission of AGN at Millimeter Wavelengths as Seen by POLAMI

Iván Agudo ^{1,*}  and Clemens Thum ²¹ Instituto de Astrofísica de Andalucía-CSIC, Glorieta de la Astronomía, E-18008 Granada, Spain² Instituto de Radio Astronomía Milimétrica, Avenida Divina Pastora, 7, Local 20, E-18012 Granada, Spain

* Correspondence: iagudo@iaa.es

Abstract: We review results from the POLAMI program, which monitors the polarization properties of 36 blazars at the IRAM 30 m telescope. We found that the variability of the degree of linear polarization is faster and of higher amplitude at 1 mm than at 3 mm and that the linear polarization is also more variable than the total flux. The linear polarization angle is highly variable in all sources with excursions $>180^\circ$; and for the case of the polarization angle, also the 1 mm variations appear to be faster than those at 3 mm. These results are fully compatible with recent multi-zone turbulent jet models, and they definitively rule out the popular single-zone models for blazars. They also further confirm that the short-wavelength (inner) emitting regions have better ordered magnetic fields than the long-wavelength ones (further downstream). Moreover, the POLAMI program has shown statistical evidence that, for most of the monitored sources, circular polarization emission is displayed the majority of the time. The circular polarization detection rate and the maximum degree of circular polarization found are comparable with previous surveys at much longer wavelengths, thus, opening a new window for circular polarization and jet composition studies in the mm range. The process generating circular polarization must not be strongly wavelength-dependent. The widespread presence of circular polarization in the POLAMI sample is likely due to Faraday conversion of the linearly polarized synchrotron radiation in the helical magnetic field of the jets. The peculiar behavior of circular polarization in 3C 66A, which we consider a hallmark of circular polarization generation by Faraday conversion in helical fields, is discussed.

Keywords: galaxies: active; galaxies: jets; quasars: general; BL Lacertae objects: general; polarization; surveys



Citation: Agudo, I.; Thum, C. The Polarized Emission of AGN at Millimeter Wavelengths as Seen by POLAMI. *Galaxies* **2022**, *10*, 87. <https://doi.org/10.3390/galaxies10040087>

Academic Editor: Jose L. Gómez

Received: 5 August 2021

Accepted: 20 July 2022

Published: 4 August 2022

Publisher's Note: MDPI stays neutral with regard to jurisdictional claims in published maps and institutional affiliations.



Copyright: © 2022 by the authors. Licensee MDPI, Basel, Switzerland. This article is an open access article distributed under the terms and conditions of the Creative Commons Attribution (CC BY) license (<https://creativecommons.org/licenses/by/4.0/>).

1. Introduction

The radio-loud class of active galactic nuclei (AGN) are characterized by powerful relativistic jets that radiate strongly at all spectral ranges from radio waves to the highest energy γ -rays. The relativistic nature of these jets, when oriented close to the line of sight (as in the case of blazars), further enhances the emitted power by relativistic Doppler boosting. The relativistic jet pointing to us then often outshines the entire host galaxy.

The AGN jet emission also shows fast total flux density and polarization variability all along the electromagnetic spectrum, e.g., [1–6]. The millimeter-range jet emission is produced by the synchrotron process, testifying to the important role that magnetic fields play in the formation of jets that are also an essential ingredient for the jet-formation mechanism, e.g., [7], as well as for the emission mechanisms, e.g., [2,4].

Observations of the polarization characteristics, therefore, provide information about the physical parameters of the magnetized plasma by breaking some degeneracies in the modeling of non-polarization data, particularly if circular polarization is observed together with linear polarization at more than one single frequency.

Observations at millimeter wavelengths scrutinizes the innermost optically thin regions of relativistic jets [8,9], therefore, offering an unaltered picture of these sources,

virtually always free of opacity effects. Furthermore, the Faraday rotation measures, which are expected to not be much larger than $\sim 10^5$ rad m^{-2} e.g., [10,11] but [12]. At short millimeter wavelengths, these rotation measures produce only small polarization angle rotations that allow measuring the polarization emissions almost unaltered from these effects.

Perhaps because of the weak circular polarization that has traditionally been detected at centimeter wavelengths, not much research has been performed regarding this relevant parameter. Previous single dish surveys were made at the Parkes telescope [13], the University of Michigan Radio Observatory [14], the Effelsberg 100 m telescope [15,16], the Arecibo telescope (R. Taylor, private communication) and the IRAM 30 m telescope [9,17]. Interferometric observations have also been performed with VLBI by the MOJAVE program [18], with connected interferometers at the VLA [19] and at ATCA [20,21].

A first attempt to make a study the variability of the four Stokes parameters (i.e., not only the total flux and linear polarization but also the circular polarization) of a relatively large sample of AGN at mm wavelengths was performed in [9]. Here, we provide a review, also containing some new data and ideas, of the main results obtained by the POLAMI (Polarimetric Monitoring of AGN at Millimeter Wavelengths¹ program; see [22–24]), at the IRAM 30 m Telescope in Granada (Spain). This program has been monitoring a set of 36 AGN at a good sampling rate since 2006.

2. The POLAMI Program

POLAMI is a long term monitoring program conducted at the IRAM 30 m telescope that observes simultaneously the total flux, the linear and circular polarization of a set of some of the brightest millimeter AGN at 86 (3.5 mm) and 229 GHz (1.3 mm); see [22] for the source list and calibrators observed. Observations are mainly made with the Observatory's EMIR receiver [25] and the XPOL 4-Stokes polarimetric procedures [26]. The program started in autumn 2006 and is expected to be active until at least the summer of 2024. Here, we report on the data collected up to the first evaluation date on 18 August 2014.

The median time sampling during this period was ~ 22 days; see also [22–24]. The source sample (which contains most of the sources included in the VLBA-BU-BLAZAR program [27] to maximize the science output of the POLAMI, the VLBA-BU-BLAZAR, and all the parallel monitoring programs along the spectral range) includes 24 flat spectrum radio quasars, 11 BL Lac objects and three radio galaxies with redshifts ranging from $z = 0.0176$ to $z = 2.218$.

Details about control of the data reduction and calibration, in particular about the evaluation of the quality of the acquired data and the instrumental polarization estimate and its correction are given in [22] (total flux), [23] (circular polarization) and [24] (linear polarization and angle). After all calibrations and corrections, a (1σ) sensitivity of 0.5% in linear polarization fraction was reached, as well as 4.7° in polarization angle and 0.23% in circular polarization 3.5 mm. At 1.3 mm, these values are typically 1.7%, 9.9° and 0.72%.

3. Results and Variability Analysis

In Figure 1, we show an example of the observational products that the POLAMI program provides systematically for every one of our monitored sources. Figure 1 shows the 3 mm data of the total flux (I), linear polarization degree (m_L), linear polarization angle (χ) and circular polarization (m_C) for one of the sources in our sample, i.e., 3C 66A. The $n\pi$ ambiguity of the polarization angle at the 3 mm wavelength was handled by rotating an angle by $n\pi$ if the difference to the weighted mean of the two immediately preceding measurements was larger than $\pi/2$, with n chosen to minimize the difference.

For 1 mm, χ was rotated by the multiple of π , which made its value as close as possible to the simultaneously observed value at 3 mm. Although the POLAMI program is still active and a database contains updated measurements for essentially every new observing session, in the following sections, we review the results from the program reported in [23,24], which cover the time period spanning from October 2006 to August 2014. More updated results are in preparation and will be published elsewhere.

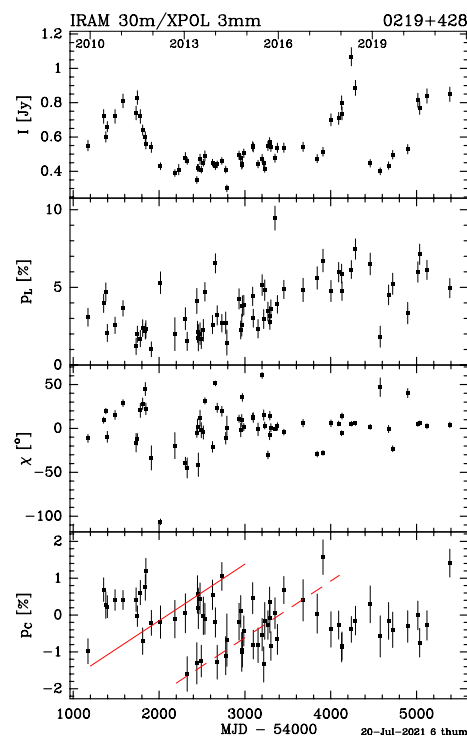


Figure 1. The POLAMI database product for the BL Lac object 3C 66A at 3 mm wavelength. The total flux (I), linear polarization degree (m_L), linear polarization angle (χ) and circular polarization (m_C) measurements (top to bottom) are shown for our POLAMI observations from the start until June 2021. The two red lines overlaid on the m_C data illustrate the m_C trains discussed in the text.

3.1. Total Flux and Spectral Index

The total flux results for the entire POLAMI sample reported in [22] show that all sources are highly variable at both 3 and 1 mm with max/min ratios ranging from ~ 2 to ≈ 42 and with median power spectral density (PSD) slopes $\beta_3 \sim 1.9$ and $\beta_1 \sim 1.6$ at 3 and 1 mm, respectively. At 3 mm, the median fractional variability amplitude² $\tilde{F}_3 \sim 0.3$, whereas at 1 mm $\tilde{F}_1 = 0.4$. \tilde{F}_1 shows larger values than \tilde{F}_3 for a given source in general, therefore, implying that bright mm AGN at 3 mm shows smaller variability amplitude than at 1 mm.

The time needed for the auto-correlation function (ACF, as defined in [24]) to drop from its maximum to zero, τ_0 , represents a characteristic time scale of the most prominent flares in the total flux data. The median τ_0 at 3 mm is 318 days for the POLAMI sample whereas, at 1 mm, τ_0 is also smaller (median value 197 days) as well. Therefore, the data show that the total flux has smaller fractional variability amplitudes and longer time-scales at 3 mm with regard to 1 mm, therefore, reflecting that the longer wavelength emission comes from a larger and less-variable region than the shorter wavelength one. This agrees with turbulent models reproducing the variability of AGN jet plasmas involving larger cell sizes at longer wavelengths, e.g., [28].

The spectral index between the short millimeter wavelengths of the POLAMI observations (α^3) is also variable and only positive in exceptionally bright flares when the spectrum is optically thick see [24]. However, for most of the time, the spectral index is negative (with the median $\tilde{\alpha} \approx -0.6$) for the studied sources; see also [9]. This is different from what is reported in cm radio observations, where the α is typically ~ 0 or positive, i.e., at least partially optically thick [15,29].

3.2. Linear Polarization Degree

The POLAMI database also shows remarkable variability in the linear polarization degree for most of the monitored sources, although the variability is clearly different from the one in total flux for all sources (see, e.g., Figure 1). m_L ranges at 3 mm from $\sim 0\%$ to

$\sim 15\%$ with median $\tilde{m}_L \approx 3\%$ for the sample, whereas, at 1 mm, the values of m_L range from $\sim 0\%$ to 16% and have a median $\tilde{m}_L \approx 6\%$. This might suggest a larger polarization degree at 1 mm than at 3 mm.

However, this effect is subject to bias resulting from the systematically higher noise at the shorter wavelength. Further evidence for the larger polarization degree at 1 mm was obtained from the study of individual observations. The ratio of 1 mm to 3 mm linear polarization degree detections made simultaneously for every observation of every source in the sample, i.e., the $m_{L,1}/m_{L,3}$ ratio presented in [24], gave median values of $m_{L,1}/m_{L,3} \sim 2.6$, hence, confirming previous studies showing that, the 1 mm linear polarization degree was, in general, larger than at 3 mm in AGN jets [9,17].

This cannot be attributed to the effect of the Rician bias on the POLAMI data, which was considered and, therefore, was compensated accordingly. Depolarization due to optical depth or Faraday depolarization is often an issue at longer wavelengths; however, it is small or negligible at our short millimeter wavelengths, even at 3 mm; see [24].

For the higher linear polarization peaks, the time scales of variability of m_L , given by τ_0 , were significantly shorter for the 1 mm data ($\tilde{\tau}_0 = 45$ days) with regard to the 3 mm data ($\tilde{\tau}_0 = 171$ days). This result was also shown to be reproduced when comparing the τ_0 at 3 and 1 mm for every given source; see [24]. Furthermore, the time scales of variability of m_L were found to be shorter than for the total flux, hence, showing that the linear polarization varies over shorter time scales than does the total flux at both 3 and 1 mm.

Once more, these findings are consistent with inhomogeneous (perhaps turbulent) jet models where the emission is produced in regions of different characteristic sizes and configurations of the magnetic field at every spectral range such that the magnetic field cells at 1 mm are better ordered, in general, than at 3 mm. Within this scenario, the faster linear polarization variability as compared with such in total flux density is produced by the cancellation of orthogonal polarization sub-cells within the same emission region at every given observing wavelength.

3.3. Linear Polarization Angle

The linear polarization angle (χ) varies strongly at 3 and 1 mm as well for all sources in the POLAMI sample, while maintaining a good general level of correspondence (within the errors) or the χ measurements at both wavelengths. A relevant aspect to study regarding the χ variability is the one of large polarization angle rotations by more than 90° . Within the POLAMI sample, 33 out of 36 targets displayed χ rotations by $\geq 90^\circ$, and 21 of them had $\geq 180^\circ$ rotations.

The numbers are similar for the case of the 1 mm polarization angles, hence, reflecting that large χ rotations are common in AGN jets. The $\geq 180^\circ$ rotations happened on time scales of the order of 80 and 150 days on average at 1 and at 3 mm, respectively, although large deviations were found from these numbers for particular sources. The standard deviations of the time scales for the $\geq 180^\circ$ swings were 368 and 208 days for the 3 and 1 mm data, respectively.

3.4. Misalignment between Linear Polarization and Jet Position Angles

The new 3 and 1 mm data sets of the polarization angle χ published in [24] are an order of magnitude larger than previous similar millimeter studies [9,17]. We, therefore, undertook a new analysis of the alignment of the instantaneous polarization direction with respect to the position angle ϕ of the inner jet. Figure 2 shows the distribution of observations with respect to the misalignment angle $|\chi - \phi|$ separately for quasars and BL Lac objects.

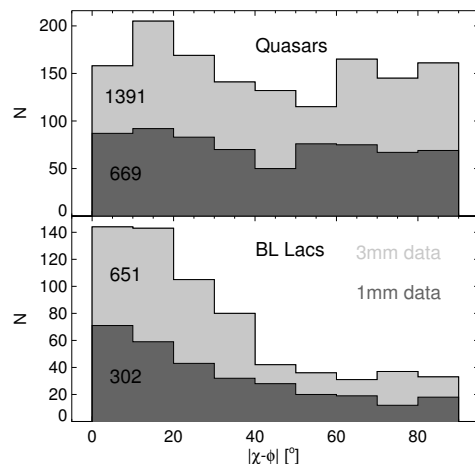


Figure 2. Misalignment between the polarization angle χ and the jet direction ϕ at 3 and 1 mm wavelengths for quasars and BL Lac objects. The polarization angle measurements were taken from [24], while the jet position angles were from [27], except for 0355+508 [30] and for 0235+164, which was taken from the VLBA–BU–BLAZAR program web page; see also [24]. The number of independent 3 and 1 mm observations are indicated for both blazar classes.

The distributions sampled over the period 2009–2014 are markedly different for the two blazar classes. While the orientation of the polarization angle is completely random for quasars, BL Lac objects display a clear preference for alignment. This finding is at variance with some previous observations at longer wavelengths (see, e.g., [31,32]) but agrees with the MOJAVE survey at 2 cm [33]. A high observing frequency and long monitoring periods may be important for bringing out this result. This may also explain why our two previous single-epoch surveys [9,17] did not find clear signs of alignment.

Two-dimensional axisymmetric models of polarized emission of blazar jets, e.g., [34] predict that the polarization angle is parallel to the jet axis or, under some restricted conditions, perpendicular to it. It, therefore, seems that BL Lac objects are compatible, to a large degree, with the idealizations used in the model, mostly cylindrical symmetry and low synchrotron optical depth. Some of these idealizations, notably the cylindrical symmetry, appear to break down in quasars. The much higher level of activity in quasars as compared with BL Lac objects demonstrated by the frequent appearance of superluminal ejections and the often distorted geometry of their jets, may favor the occurrence of numerous shocks, which may make any angle with the overall jet direction. Alignment is then quickly lost.

Closer inspection of the POLAMI data for BL Lac objects shows that the dominance of small misalignment angles $|\chi - \phi|$ is due to 7 out of 11 sources—namely, 0219+428, 0829+046, 0851+202, 0954+658, 1101+384, 1219+285 and 2200+420. The remaining four sources have rather flat distributions as with those of most quasars. On the other hand, there is a minority of quasars in the sample—namely, 0336–019, 0836+710, 1222+216, 1226+023 and 1641+399, which have distributions with peaks at $|\chi - \phi|$ near zero, except for 1226+023, which has peaks near 90° .

We, therefore, conclude that the type of alignment behavior, random or peaked, is not primarily related with the blazar class, although we stress again that BL Lac objects have clearer tendency to align at $|\chi - \phi|$ close to zero. We postulate that the physical reason for the distinct alignment behavior of quasars and BL Lac objects may lie in the dominance of shocks in the jet structure, which appears to be more pronounced in quasars as compared to BL Lac objects. If this is the case, in our current POLAMI data set, shocks dominate the jet structure in 30% of the BL Lac objects and in 70% of the quasars.

3.5. Rotation Measure between 3 and 1 mm

An estimate of the 3 to 1 mm rotation measures (RM, as measured for every source and for every observing epoch), by taking advantage the simultaneity of the 3 and 1 mm polarization observations in the POLAMI program, was also made [24]. However, the propagated errors in the computation of RM, of the order of $\sim 2 \times 10^4 \text{ rad m}^{-2}$, prevented the provision of any information about the variability of RM. Nonetheless, the POLAMI team is in the position to set constraints on the typical RM values from the POLAMI data. The results show that the measured RM values are $\lesssim 10^5 \text{ rad m}^{-2}$, which is consistent with other RM measurements measured at longer wavelengths in the literature [10,11,35–39] but [12].

3.6. Relation between the Total Flux, Linear Polarization Degree and Polarization Angle Variability

A simple visual inspection of Figure 1 and those corresponding the all remaining sources in the POLAMI sample reveals that, except for extremely prominent flares; where all emission by a source might be driven by a single isolated emission zone, there is no general correlation of the total flux and the linear polarization parameters at either 3 or 1 mm, thus, reflecting that I , m_L and χ follow independent evolutions. This has been formally checked by correlation studies; see [24].

For the emission at a given observing wavelength coming from a single emission zone, the I , m_L and χ data trains should behave in a coherent and correlated way. The fact that a completely different behavior has been observed, in general, for all sources in the POLAMI sample indicates that the emission in bright millimeter AGN jets should come from at least two (likely more) emission zones, which is in line with previous evidence presented in support of inhomogeneous and dynamic plasmas in AGN jets, e.g., such as those reproduced by turbulence models.

3.7. Circular Polarization

The POLAMI program has acquired 2728 observations at the 3 mm wavelength of circular polarization (m_C) up to 18 August 2014. These data are shown and discussed in detail in [23].

The main results, of which many are directly visible in Figure 3, are that (1) all but one sources of the sample were detected in m_C —most of them several times; (2) the distribution of the observed m_C values of most sources as well as of the whole sample is broader than that of the calibrators; (3) the highest m_C detected, 2%, and the detection rate are comparable to previous surveys at centimeter wavelengths; (4) in most sources where m_C was detected more than 10 times, the sign of m_C is variable, only a minority of seven sources have a strong sign preference, and among these seven sources, three of them were already known to show this behavior; (5) circular and linear polarization are not correlated in general; and (6) the time scale of m_C variations is on the order of, or faster than, our typical sampling interval of 1 month. Nonetheless, in a few sources, we detect coherent evolution of m_C on time scales of 1 year.

Based on findings 1 and 2, the striking result of this large 3 mm survey is that circular polarization is widespread among the blazar population. This is shown not only by the m_C detection in virtually all sources but also by the statistics of the large number of m_C measurements. They permit an accurate determination of the width of the m_C distribution, which is found to be larger for AGN than for the unpolarized calibrators (see Figure 3). Clearly, weak m_C of order $\lesssim 0.5\%$ is present in most sources most of the time.

The high maximum degree of circular polarization and the high detection rate outlined in finding 3 constituted another surprise, since the simplest models for the creation of m_C predict a strong decrease of m_C with decreasing wavelength. In particular, this is the case for synchrotron radiation and for the intrinsic Faraday conversion of linear into circular polarization in homogeneous jets [40]. Motivated by the widespread presence of m_C and by the increasing evidence for helical magnetic fields in blazar jets, [23] suggested that most of the observed m_C is generated by extrinsic Faraday conversion where the linear polarization

emitted in one region of the jet is partially converted to m_C in a downstream region with a different orientation of its magnetic field.

However, contributions by intrinsic circular polarization cannot be excluded owing to the softer dependence of this mechanism on wavelength, which may allow intrinsic circular polarization radiation lead at high frequencies; see [40]. Finding 4 is particularly well illustrated by the m_C distribution of 0316+413, the radio galaxy 3C84, which is systematically offset to negative m_C ; see Figure 3 and [23]. Something similar happens for a small set of an additional six sources, which were observed to have a strong preference for positive or negative m_C [23].

This group of "unipolar" sources constitutes, however, less than one third of our sample. There is strong evidence that many of the other sources change their sign of m_C during the 7 year observing period reported in [23]. Such sign changes occur in synchrotron radiation if the line-of-sight magnetic field changes direction. In the favored mechanism of extrinsic Faraday conversion, sign changes are a natural consequence when the angle between the magnetic fields projected on the sky plane in the emitting and converting regions changes sign.

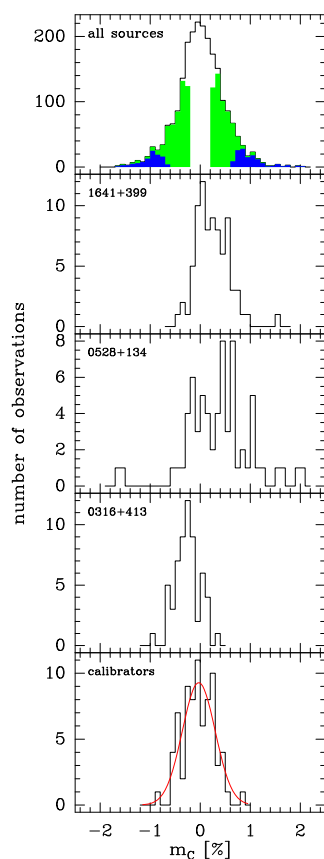


Figure 3. Distribution of 3 mm measurements of circular polarization, m_C , of a few selected sources, the calibrators and of all data in our sample (2261 valid observations). In the top frame, blue and green colors code measurements with signal-to-noise ratios greater than 3 and 1, respectively. The red curve is a Gaussian fit to the calibrator measurements.

Despite our favoring of external Faraday conversion for the creation of circular polarization, significant correlation between linear and circular polarization is not observed in the full data set [23] (Figure 5). We suggest that this is a consequence of the generally low signal-to-noise of the m_C values coupled with a low conversion efficiency. For example, an efficiency of 8% (see below) converts a typical observation of 5% linear to 0.4% circular polarization, which is at, or below, our detection threshold.

This does not prevent, however, our detection of a correlation in few events of short duration (see below), which are heavily diluted and thus not visible when the full data set is plotted. Circular polarization appears to vary rapidly. A representative example is the quasar 0528+134, which was detected 16 times during the 7 year monitoring period, Figure 3. All 16 detections are well isolated in time, separated by extended periods when m_C was below the detection threshold. The POLAMI database contains only one single case, 0836+710 during 2007–2008 when detections at $\sigma \gtrsim 3$ were made contiguously in time. The variability time scale of the bulk of the 3 mm m_C data is, thus, found to be of order of our sampling interval of $\lesssim 1$ month or shorter.

The time coherent evolution of m_C is observed in a few sources during limited periods of time. A noteworthy example is the quasar 1127–145 whose linear polarization underwent a nearly 1 year long outburst peaking on 2003.1 at $m_L \sim 10\%$. During this period, m_C displayed a significant increase marked by 12 observations of $m_C \sim 0.8\%$ of which six were detections at 3σ and one at 5σ . The Faraday conversion efficiency was of order 8% for this rather singular event. A few more events of time-coherent m_C evolution were detected, which will be discussed in separate papers.

4. Discussion and Conclusions

The results presented in the previous sections can be summarized as follows: (a) the shorter millimeter wavelength emission appears to come from smaller regions with progressively better magnetic field orders, (b) one-zone models are excluded to reproduce the general properties of millimeter polarization of blazars, (c) blazar jets cannot be axisymmetric in general, at least regarding their polarization emission, (d) there are hints of fast circular polarization variability and frequent sign changes, in general, on the POLAMI data, and (e) circular polarization appears to be present in blazars at millimeter wavelengths, in general, at levels $\leq 2\%$.

The majority of these results conform with previous paradigms for millimeter emissions in blazar jets, e.g., [41], although slight modifications of this paradigm are needed to account for the general results that the POLAMI program has provided. These include that blazar jets need to be only slightly more non-axisymmetric than traditionally considered in order to explain the variability of the polarization emission. Furthermore, the prominent emission features that are visible in blazar jets at a given time should perhaps be more than one and likely do not cover the entire cross section of the jet.

We propose that the widespread occurrence of circular polarization in blazar jets at short millimeter wavelengths can be explained by the Faraday conversion of linear polarization into circular polarization from large-scale and well-ordered helical magnetic fields threading the jets. This should be combined with inhomogeneous dynamic processes to explain the short time scale of variability in circular polarization. Intrinsic circular polarization production can also explain the POLAMI circular polarization data. This possibility cannot still be excluded without a detailed modeling of a significant population of sources.

How do we expect unequivocal evidence for a Faraday conversion origin of circular polarization in helical fields to look? Optimum observing conditions may occur in a source where the helical geometry is well developed and not disturbed by rapidly traveling shocks or by other jet bending forces. This tends to narrow down the candidates to BL Lac objects, particularly those of low activity, i.e., few if any superluminal ejection events. The intermediate frequency peaked BL Lac object 3C 66A (Figure 1) is among the sources that satisfy these conditions.

The flux density of this source evolved rather smoothly between the two outburst in 2011 and 2018, suggesting that the jet emissions during this period were dominated by plasma freely streaming along the field lines. Circular polarization during this period of quiescence displayed rather peculiar behavior, only clearly seen once in the POLAMI database, following two parallel trains, each crossing zero and being coherent during about 3 years.

The simplest interpretation of this phenomenon is that the linearly polarized radiation from a stationary source, likely the core of the jet, passes through a plasma cloud whose embedded magnetic field smoothly rotates in the clockwise direction. Circular polarization increasing from negative to positive values is, thus, generated through Faraday conversion, while the circular polarization is zero when the fields of the plasma cloud and the core are aligned.

We envisage that the field rotation is simply due to the motion of the plasma cloud along a helical path. Our observation of two (or more) circular polarization trains indicate that the scenario is actually more complicated, involving more than one plasma cloud traveling along different but stable helical paths. We suggest that this event caught by POLAMI in 3C 66A constitutes the hallmark of circular polarization generation by Faraday conversion in helical fields. The details are being investigated for a forthcoming paper.

5. Outlook

The POLAMI program has accumulated 2728 observations during its first 7 years up to the first evaluation date in August 2014. Additional 2428 more observations have been made since then up to mid-May 2021. Recently, three more years of monitoring time have been granted at the IRAM 30 m Telescope, at the end of which we expect a total of more than 6200 valid observations. The key benefit of the exceptionally long duration is, apart from obtaining a precise statistical overview of the polarization properties of the blazar population, the chance to witness special events which throw new light on jet physics. Two such events have been recorded during the first 7 years, and a few more since then. Also, for the phase of the POLAMI program since mid-2021, the source sample has been partly modified to help addressing new scientific challenges in the field of high energy astrophysics, e.g., the origin of high energy extragalactic neutrinos detected by current TeV particle detectors, and the composition of extragalactic relativistic jets and their energetics.

It is an essential aspect that POLAMI operates simultaneously in full polarimetric mode and at 3 and 1 mm wavelength, the shortest wavelengths of any blazar monitoring program. Also, the current POLAMI program involves a new Target of Opportunity mode component that will make possible to quickly react to alerts or rapid and unpredicted blazar events of special interest. This, combined with the planned multi-waveband total flux and polarization coverage (wherever possible) from a number of the main astronomical facilities across the spectrum, around the globe, and in orbit makes the POLAMI program a remarkably useful tool for blazar studies. Indeed, in 2022, a series of POLAMI observations were synchronized with observations of the Imaging X-ray Polarimetry Explorer (IXPE) satellite.

We have pointed out above that the circular polarization observations of POLAMI are severely sensitivity limited. The circular polarization histogram with all sources combined (Figure 3, top frame) indeed suggests that the bulk of the sources may become detectable in circular polarization much more often if the sensitivity would be increased by a factor 2. This appears quite possible when some of the upgrades under discussion of the IRAM 30 m telescope take place. The most important and decisive component is the backend which performs the cross-correlation between the orthogonally linearly polarized receivers and thus giving Stokes V. The currently used backend VESPA limits the bandwidth used in practice to 500 MHz, much less than the bandwidth of 4 GHz of the receivers. Modern digital backends can handle such large bandwidths, e.g., [42], which may result with XPOL in even a factor 3 gain in sensitivity. A further planned upgrade at the IRAM 30 m Telescope is the installation of an array of receivers for wide field of view imaging. Although our sources are all point-like, the off-axis pixels of the array will give an improved control on instrumental polarization and atmospheric disturbances. The third component of the planned upgrade concerns an improvement of the telescope surface and its thermal behavior. We expect this to result in an improved stability of the 1 mm instrumental polarization, probably enabling the first detections of circular polarization at 1 mm. This is of great scientific interest because information on the *spectrum* of the short-mm circular

polarization will then be available for the first time. The wavelength dependence of circular polarization is the primary tool for discriminating between emission mechanisms.

Author Contributions: The two authors jointly prepared, revised, read and agreed to the published version of the manuscript. All authors have read and agreed to the published version of the manuscript.

Funding: I.A. acknowledges financial support from the Spanish “Ministerio de Ciencia e Innovación” (MICINN) through the “Center of Excellence Severo Ochoa” award for the Instituto de Astrofísica de Andalucía-CSIC (SEV-2017-0709). The POLAMI program was supported in part by MICINN through grants AYA2016-80889-P and PID2019-107847RB-C44.

Acknowledgments: The POLAMI observations were performed at the IRAM 30 m Telescope. IRAM is supported by INSU/CNRS (France), MPG (Germany) and IGN (Spain).

Conflicts of Interest: The authors declare no conflict of interest.

Notes

¹ <http://polami.iaa.es> (accessed on 19 July 2022).

² See [24] for the actual definition of fractional variability amplitude used here.

³ Defined as $\alpha = \ln(I_3/I_1)/\ln(86/229)$, where I_3 and I_1 are the simultaneous 3 and 1 mm (86 and 229 GHz, respectively) total fluxes.

References

- Marscher, A.P.; Jorstad, S. G.; D’Arcangelo, F.D.; Smith, P.S.; Williams, G.G.; Larionov, V.M.; Oh, H.; Olmstead, A.R.; Aller, M.F.; Aller, H.D.; et al. The inner jet of an active galactic nucleus as revealed by a radio-to-gamma-ray outburst. *Nature* **2008**, *452*, 966. [CrossRef]
- Marscher, A.P.; Jorstad, S.G.; Larionov, V.M.; Aller, M.F.; Aller, H.D.; Lähteenmäki, A.; Agudo, I.; Smith, P.S.; Gurwell, M.; Hagen-Thorn, V. A; et al. Probing the Inner Jet of the Quasar PKS 1510-089 with Multi-Waveband Monitoring During Strong Gamma-Ray Activity. *Astrophys. J. Lett.* **2010**, *710*, L126. [CrossRef]
- Abdo, A.A. [Fermi Collaboration] A change in the optical polarization associated with a gamma-ray flare in the blazar 3C279. *Nature* **2010**, *463*, 919.
- Agudo, I.; Marscher, A.P.; Jorstad, S.G.; Larionov, V.M.; Gómez, J.L.; Lähteenmäki, A.; Smith, P.S.; Nilsson, K.; Readhead, A.C.S.; Aller, M.F.; et al. On the Location of the Gamma-Ray Outburst Emission in the BL Lacertae Object AO 0235+164 Through Observations Across the Electromagnetic Spectrum. *Astrophys. J. Lett.* **2011**, *735*, L10. [CrossRef]
- Aleksić, J. [MAGIC Collaboration.] Unprecedented study of the broadband emission of Mrk 421 during flaring activity in March 2010. *Astron. Astrophys.* **2015**, *578*, A22. [CrossRef]
- Casadio, M.; Gómez, J.L.; Jorstad, S.G.; Marscher, A.P.; Larionov, V.M.; Smith, P.S.; Gurwell, M.A.; Lähteenmäki, A.; Agudo, I.; Molina; et al. A Multi-wavelength Polarimetric Study of the Blazar CTA 102 during a Gamma-Ray Flare in 2012. *Astrophys. J.* **2015**, *813*, 51. [CrossRef]
- Tchekhovskoy, A. Launching of Active Galactic Nuclei Jets. In *The Formation and Disruption of Black Hole Jets*; Contopoulos, I., Gabuzda, D., Kylafis, N., Eds.; Springer: Cham, Switzerland, 2015; Volume 414, pp. 45–82.
- Jorstad, S.G.; Marscher, A.P.; Stevens, J.A.; Smith, P.S.; Forster, J.R.; Gear, W.K.; Cawthorne, T.V.; Lister, M.L.; Stirling, A.M.; Gómez, J.L.; et al. Multiwaveband Polarimetric Observations of 15 Active Galactic Nuclei at High Frequencies: Correlated Polarization Behavior. *Astron. J.* **2007**, *134*, 799. [CrossRef]
- Agudo, I.; Thum, C.; Gómez, J.L.; Wiesemeyer, H. A simultaneous 3.5 and 1.3mm polarimetric survey of active galactic nuclei in the northern sky. *Astron. Astrophys.* **2014**, *566*, A59. [CrossRef]
- Zavala, R.T.; Taylor, G.B. A View through Faraday’s Fog. II. Parsec-Scale Rotation Measures in 40 Active Galactic Nuclei. *Astrophys. J.* **2004**, *612*, 749. [CrossRef]
- Hovatta, T.; Lister, M.L.; Aller, M.F.; Aller, H.D.; Homan, D.C.; Kovalev, Y.Y.; Pushkarev, A.B.; Savolainen, T. MOJAVE: Monitoring of Jets in Active Galactic Nuclei with VLBA Experiments. VIII. Faraday Rotation in Parsec-scale AGN Jets. *Astron. J.* **2012**, *144*, 105. [CrossRef]
- Martí-Vidal, I.; Muller, S.; Vlemmings, W.; Horellou, C.; Aalto, S. A strong magnetic field in the jet base of a supermassive black hole. *Science* **2015**, *348*, 311. [CrossRef] [PubMed]
- Komesaroff, M.M.; Roberts, J.A.; Milne, D.K.; Rayner, P.T.; Cooke, D.J. Circular and linear polarization variations of compact radio sources. *Mon. Not. R. Astron. Soc.* **1984**, *208*, 409. [CrossRef]
- Aller, H.D.; Aller, M.F.; Plotkin, R.M. Circular Polarization Variability in Extragalactic Sources on Time Scales of Months to Decades. *Astrophys. Space Sci.* **2003**, *288*, 17–28. [CrossRef]

15. Fuhrmann, L.; Angelakis, E.; Zensus, J. A.; Nestoras, I.; Marchili, N.; Pavlidou, V.; Karamanavis, V.; Ungerechts, H.; Krichbaum, T. P.; Larsson, S.; et al. The F-GAMMA programme: Multi-frequency study of active galactic nuclei in the Fermi era. Programme description and the first 2.5 years of monitoring. *Astron. Astrophys.* **2016**, *596*, A45. [[CrossRef](#)]
16. Myserlis, I.; Angelakis, E.; Kraus, A.; Fuhrmann, L.; Karamanavis, V.; Zensus, J. Physical Conditions and Variability Processes in AGN Jets through Multi-Frequency Linear and Circular Radio Polarization Monitoring. *Galaxies* **2016**, *4*, 58. [[CrossRef](#)]
17. Agudo, I.; Thum, C.; Wiesemeyer, H.; Krichbaum, T.P. A 3.5 mm Polarimetric Survey of Radio-loud Active Galactic Nuclei. *Astrophys. J. Suppl. Ser.* **2010**, *189*, 1. [[CrossRef](#)]
18. Homan, D.C.; Lister, M.L. MOJAVE: Monitoring of Jets in Active Galactic Nuclei with VLBA Experiments. II. First-Epoch 15 GHz Circular Polarization Results. *Astron. J.* **2006**, *131*, 1262. [[CrossRef](#)]
19. Bower, G.C.; Falcke, H.; Mellon, R.R. A Radio Survey for Linear and Circular Polarization in Low-Luminosity Active Galactic Nuclei. *Astrophys. J.* **2002**, *578*, L103. [[CrossRef](#)]
20. Rayner, D.P.; Norris, R.P.; Sault, R.J. Radio circular polarization of active galaxies. *Mon. Not. R. Astron. Soc.* **2000**, *319*, 484–496. [[CrossRef](#)]
21. O’Sullivan, S.P.; McClure-Griffiths, N.M.; Feain, I.J.; Gaensler, B.M.; Sault, R.J. Broad-band radio circular polarization spectrum of the relativistic jet in PKS B2126-158. *Mon. Not. R. Astron. Soc.* **2013**, *435*, 311–319. [[CrossRef](#)]
22. Agudo, I.; Thum, C.; Molina, S.N.; Casadio, C.; Wiesemeyer, H.; Morris, D.; Paubert, G.; Gómez, J.L.; Kramer C. POLAMI: Polarimetric Monitoring of AGN at Millimetre Wavelengths - I. The programme, calibration and calibrator data products. *Mon. Not. R. Astron. Soc.* **2018**, *474*, 1427–1435. [[CrossRef](#)]
23. Thum, C.; Agudo, I.; Molina, S.N.; Casadio, C.; Gómez, J.L.; Morris, D.; Ramakrishnan, V.; Sievers, A. POLAMI: Polarimetric Monitoring of Active Galactic Nuclei at Millimetre Wavelengths - II. Widespread circular polarization. *Mon. Not. R. Astron. Soc.* **2018**, *473*, 2506–2520. [[CrossRef](#)]
24. Agudo, I.; Thum, C.; Ramakrishnan, V.; Molina, S.N.; Casadio, C.; Gómez, J.L. POLAMI: Polarimetric Monitoring of Active Galactic Nuclei at Millimetre Wavelengths - III. Characterization of total flux density and polarization variability of relativistic jets. *Mon. Not. R. Astron. Soc.* **2018**, *473*, 1850–1867. [[CrossRef](#)]
25. Carter, M.; Lazareff, B.; Maier, D.; Chenu, J. -Y.; Fontana, A. -L.; Bortolotti, Y.; Boucher, C.; Navarrini, A.; Blanchet, S.; Greve, A.; et al. The EMIR multi-band mm-wave receiver for the IRAM 30-m telescope. *Astron. Astrophys.* **2012**, *538*, A89. [[CrossRef](#)]
26. Thum, C.; Wiesemeyer, H.; Paubert, G.; Navarro, S.; Morris, D. XPOL?the Correlation Polarimeter at the IRAM 30-m Telescope. *Publ. Astron. Soc. Pac.* **2008**, *120*, 777. [[CrossRef](#)]
27. Jorstad, S.G.; Marscher, A.P.; Morozova, D.A.; Troitsky, I.S.; Agudo, I.; Casadio, C.; Foord, A.; Gómez, J.L.; MacDonald, N.R.; Molina, S.N.; et al. Kinematics of Parsec-scale Jets of Gamma-Ray Blazars at 43 GHz within the VLBA-BU-BLAZAR Program. *Astrophys. J.* **2017**, *846*, 98. [[CrossRef](#)]
28. Marscher, A.P. Turbulent, Extreme Multi-zone Model for Simulating Flux and Polarization Variability in Blazars. *Astrophys. J.* **2014**, *780*, 87. [[CrossRef](#)]
29. Angelakis, E. Fuhrmann, L.; Nestoras, I.; Fromm, C.M.; Perucho-Pla, M.; Schmidt, R.; Zensus, J.A.; Marchili, N.; Krichbaum, T.P.; Ungerechts, H.; et al. F-GAMMA: On the phenomenological classification of continuum radio spectra variability patterns of Fermi blazars. *J. Phys. Conf. Ser.* **2012**, *372*, 012007. [[CrossRef](#)]
30. Molina, S.N.; Agudo, I.; Gómez, J.L.; Krichbaum, T.P.; Martí-Vidal, I.; Roy, A.L. Evidence of internal rotation and a helical magnetic field in the jet of the quasar NRAO 150. *Astron. Astrophys.* **2014**, *566*, A26. [[CrossRef](#)]
31. Gabuzda, D.C.; Pushkarev, A.B.; Cawthorne, T.V. Analysis of lambda=6cm VLBI polarization observations of a complete sample of northern BL Lacertae objects. *Mon. Not. R. Astron. Soc.* **2000**, *319*, 1109. [[CrossRef](#)]
32. Pollack, L.K.; Taylor, G.B.; Zavala, R.T. VLBI Polarimetry of 177 Sources from the Caltech-Jodrell Bank Flat-Spectrum Survey. *Astrophys. J.* **2003**, *589*, 733. [[CrossRef](#)]
33. Lister, M.L. Parsec-Scale Jet Polarization Properties of a Complete Sample of Active Galactic Nuclei at 43 GHz. *Astrophys. J.* **2001**, *562*, 208. [[CrossRef](#)]
34. Lyutikov, M.; Pariev, V.I.; Gabuzda, D.C. Polarization and structure of relativistic parsec-scale AGN jets. *Mon. Not. R. Astron. Soc.* **2005**, *360*, 869–891. [[CrossRef](#)]
35. Gabuzda, D.C.; Knuettel, S.; Reardon, B. Transverse Faraday-rotation gradients across the jets of 15 active galactic nuclei. *Mon. Not. R. Astron. Soc.* **2015**, *450*, 2441–2450. [[CrossRef](#)]
36. Gómez, J.L.; Marscher, A.P.; Jorstad, S.G.; Agudo, I.; Roca-Sogorb, M. Faraday Rotation and Polarization Gradients in the Jet of 3C 120: Interaction with the External Medium and a Helical Magnetic Field? *Astrophys. J.* **2008**, *681*, L69 [[CrossRef](#)]
37. Gómez, J. L.; Roca-Sogorb, M.; Agudo, I.; Marscher, A.P.; Jorstad, S.G. On the Source of Faraday Rotation in the Jet of the Radio Galaxy 3C 120. *Astrophys. J.* **2011**, *733*, 11. [[CrossRef](#)]
38. Hovatta, T.; O’Sullivan, S.; Martí-Vidal, I.; Savolainen, T.; Tchekhovskoy, A. Magnetic field at a jet base: extreme Faraday rotation in 3C 273 revealed by ALMA. *Astron. Astrophys.* **2019**, *623*, A111. [[CrossRef](#)]
39. Kravchenko, E.V.; Kovalev, Y.Y.; Sokolovsky, K.V. Parsec-scale Faraday rotation and polarization of 20 active galactic nuclei jets. *Mon. Not. R. Astron. Soc.* **2017**, *467*, 83. [[CrossRef](#)]
40. Wardle J.F.C.; Homan, D.C. Theoretical Models for Producing Circularly Polarized Radiation in Extragalactic Radio Sources. *Astrophys. Space Sci.* **2003**, *288*, 143–153. [[CrossRef](#)]

41. Marscher, A.P. Variability of Blazars and Blazar Models over 38 Years. *Galaxies* **2016**, *4*, 37. [[CrossRef](#)]
42. Torne, P.; Desvignes, G.; Eatough, R.P.; Karuppusamy, R.; Paubert, G.; Kramer, M.; Cognard, I.; Champion, D.J.; Spitler, L.G. Detection of the magnetar SGR J1745-2900 up to 291 GHz with evidence of polarized millimetre emission. *Mon. Not. R. Astron. Soc.* **2017**, *465*, 242. [[CrossRef](#)]